Nonlocal and Nonadiabatic Effects in the Charge-Density Response of Solids: A Time-Dependent Density-Functional Approach

Martin Panholzer,[1,2,*] Matteo Gatti,[1,2,3] and Lucia Reining[1,2]
[1]*Laboratoire des Solides Irradiés, École Polytechnique, CNRS, CEA, Université Paris-Saclay, F-91128 Palaiseau, France*
[2]*European Theoretical Spectroscopy Facility (ETSF)*
[3]*Synchrotron SOLEIL, L'Orme des Merisiers, Saint-Aubin, BP 48, F-91192 Gif-sur-Yvette, France*

(Received 25 July 2017; revised manuscript received 15 February 2018; published 20 April 2018)

The charge-density response of extended materials is usually dominated by the collective oscillation of electrons, the plasmons. Beyond this feature, however, intriguing many-body effects are observed. They cannot be described by one of the most widely used approaches for the calculation of dielectric functions, which is time-dependent density functional theory (TDDFT) in the adiabatic local density approximation (ALDA). Here, we propose an approximation to the TDDFT exchange-correlation kernel which is nonadiabatic and nonlocal. It is extracted from correlated calculations in the homogeneous electron gas, where we have tabulated it for a wide range of wave vectors and frequencies. A simple mean density approximation allows one to use it in inhomogeneous materials where the density varies on a scale of 1.6 r_s or faster. This kernel contains effects that are completely absent in the ALDA; in particular, it correctly describes the double plasmon in the dynamic structure factor of sodium, and it shows the characteristic low-energy peak that appears in systems with low electronic density. It also leads to an overall quantitative improvement of spectra.

DOI: 10.1103/PhysRevLett.120.166402

The response to an external perturbation is an important tool to probe materials, and spectroscopic experiments play a crucial role [1]. Response properties are also of interest for applications: examples are the linear response to photons, which governs optical properties and, hence, the color of materials and their capability to absorb the sunlight, or the response to a beam of fast charges, which determines the stopping power [2]. A first attempt to interpret experimental findings or to predict response properties is based on the band structure, in an independent-particle picture. However, collective effects and signatures of strong correlation influence and sometimes even dominate electronic spectra, making their calculation a formidable intellectual challenge and a crucial tool for technological applications. In optical absorption spectra, the Coulomb interaction can lead to bound electron-hole pairs that create sharp excitonic peaks in the fundamental gap [3]. Other important spectroscopic quantities are the loss function and the dynamic structure factor as measured in electron energy loss spectroscopy or inelastic x-ray scattering (IXS) [1]; for example, the loss function exhibits the plasmon excitations and is, therefore, a key ingredient for plasmonics [4]. It is also crucial for theory, since the density-density response function enters the calculation of the correlation energy in the adiabatic connection formula [5,6], and it is one of the main building blocks of many-body perturbation theory [7].

At first sight, spectra are often dominated by classical electrostatic (Hartree) effects for which the random phase approximation (RPA) is sufficient to capture the essential trends [1]. Beyond the RPA, the adiabatic local density approximation (ALDA) to time-dependent density functional theory (TDDFT) yields, in general, a small quantitative improvement [8]. However, often, the resulting rough overall agreement is not sufficient for today's needs. Details of the loss function are responsible for the shape of the satellite spectra in photoemission and, therefore, transmit precious information, for example, about doping [9]. Especially in correlated materials, even weak low-energy structures can dramatically influence materials properties [10]. Loss spectra can exhibit many-body effects such as lifetime broadening [11,12] or double-plasmon excitations [13,14], and in the low-density regime, the spectral shape can be very different from the naively expected single plasmon peak, even in the homogeneous electron gas (HEG) [15]. To capture those intriguing effects, one has to go beyond the RPA and ALDA. Many advanced density functionals have been developed which can be directly applied to real materials; some of them are nonlocal [16–18], others are nonadiabatic [19–21]. However, most of them are meant to improve just one of the shortcomings of the ALDA; for example, long-range corrected functionals are often adiabatic [22–25]. On the other side, more advanced calculations in the TDDFT framework exist in the HEG [15,26–29] but without an indication of how to use them in a real material. Interestingly, even beyond density functionals, nonadiabatic effects are difficult to capture; in particular, the widely used Bethe-Salpeter equation within

many-body perturbation Green's function theory is usually applied in an adiabatic approximation [3].

The aim of the present work is to close this gap by introducing a general strategy: in the spirit of ground-state density functionals, such as the LDA [30], our strategy consists of two parts: first, an advanced calculation in the HEG, and second, a "connector," namely, a prescription of how to use the result in real materials. The enormous advantage of such a procedure is that the advanced calculation is done only once and forever; indeed, our HEG results are freely available [31]. By using the very simple connector proposed in this work, results for real materials are then obtained with a computational effort that is similar to the RPA. They show features that are extremely difficult to obtain otherwise, in particular, double-plasmon excitations and the double-peak structure which characterize strong correlation in the low-density regime.

For an illustration, we concentrate on sodium as a prototype material. Fig. 1 shows experimental [40,41] and various theoretical results for a moderate momentum transfer. In agreement with literature [40,41], the RPA dynamic structure factor exhibits one plasmon peak that is blue shifted with respect to experiment. The ALDA moves spectral weight to lower energies. However, compared to experiment, the plasmon energy is still too large, and the peak is too asymmetric. Moreover, the double plasmon, which is clearly visible in experiment around 12 eV, is completely absent. In order to improve the spectral shape, one can, *ad hoc*, add quasiparticle lifetime corrections

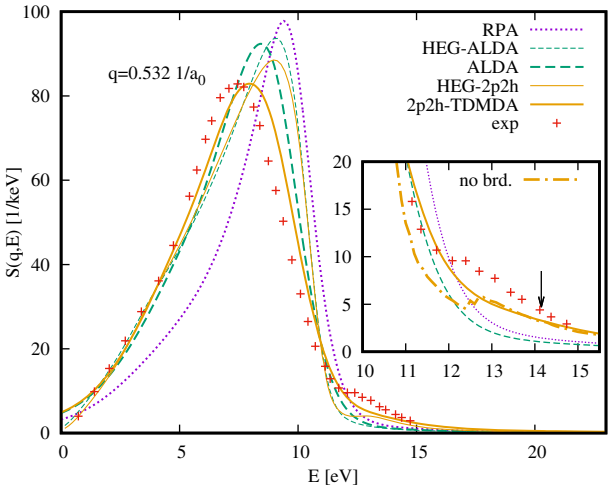

FIG. 1. The dynamic structure factor of sodium at $q = 0.531/a_0$: experimental IXS results of Ref. [40] (red crosses) and different levels of theory for the HEG at $r_s = 4$, namely ALDA (thin dashed green curve) and $2p2h$ (thin yellow solid curve) and for the real material, namely RPA (purple short-dashed curve), ALDA (green dashed curve) and $2p2h$ (yellow solid curve). Inset: zoom on the double plasmon, in particular $2p2h$ (yellow curve) with (solid curve) and without (dotted-dashed curve) Gaussian broadening. Arrow: energy of the double plasmon in Ref. [13].

[40,41], but even this empirical procedure cannot yield the double plasmon. The latter has been calculated diagrammatically in the HEG by Sturm and Gusarov [42], and qualitative agreement with experiment was found [13]. A finer comparison is hindered by the fact that, even in sodium, the effects of the crystal are not negligible: Fig. 1 shows that the ALDA result for the HEG is significantly different from the ALDA in sodium. In order to distinguish effects of the crystal from the description of many-body effects, let us first look at the HEG.

The first task is to calculate the density-density response function $\chi(q, \omega, n)$, which is a function of wave vector q, frequency ω, and the homogeneous density n, on a level of theory that includes correlations and the explicit coupling of excitations sufficiently well. A suitable starting point is the correlated equations of motion approach of Böhm *et al.* [43]. It relies on a Jastrow correlated ground state $|\psi_0\rangle = F|\phi_0\rangle/\mathcal{N}$, where ϕ_0 is a Hartree-Fock ground state and $\mathcal{N}$ is the normalization. F is the correlation operator. When restricting it to two particle correlations, it reads $F = e^{\frac{1}{2}\sum_{i<j} u(\mathbf{r}_i - \mathbf{r}_j)}$. The correlation functions u are found by minimization of the energy. Excited states are described by neutral excitations of $|\phi_0\rangle$, while F is kept constant. In this work, single particle hole and two-particle two-hole ($2p2h$) excitations are included. These excitations are optimized by employing the least-action principle. For the calculation of χ, we need matrix elements involving the correlated excited states. This is done within the correlated basis functions formalism [44,45]. The static structure function $S(q)$ appears as a fundamental ingredient in the result, while the explicit knowledge of u is not needed. Therefore, we can profit from Monte Carlo (MC) calculations, which yield $S(q)$ with high precision [46], whereas in general, they do not access spectra. Compared to the original work [43], here, we use a more complete description of the pair propagator, which improves the quality of the result but which is not crucial for the main purpose of this Letter. The improved method, which we denote $2p2h$, is described in detail in Ref. [47].

Figure 2 shows typical $\chi(q, \omega, n)$ for $q = 2.2k_F$ (where k_F is the Fermi wave vector) and n corresponding to $r_s = 8$. The RPA shows a broad and featureless plasmon excitation around 5.5 eV. This can be compared to the more realistic result of Takada [15], which has been obtained with an improved version of the Richardson-Ashcroft exchange-correlation kernel [29]. This kernel, which satisfies many exact conditions, is wave vector and frequency dependent. However, it has been derived for imaginary frequencies, and while it yields significant improvement in correcting RPA correlation energies [48], its performance for spectroscopy is less obvious. Thus, we expect that the observed corrections with respect to the RPA are relevant, while there may still be small deviations from the (unknown) exact spectrum. In any case, today, Takada's result probably represents the best available benchmark. It is remarkably

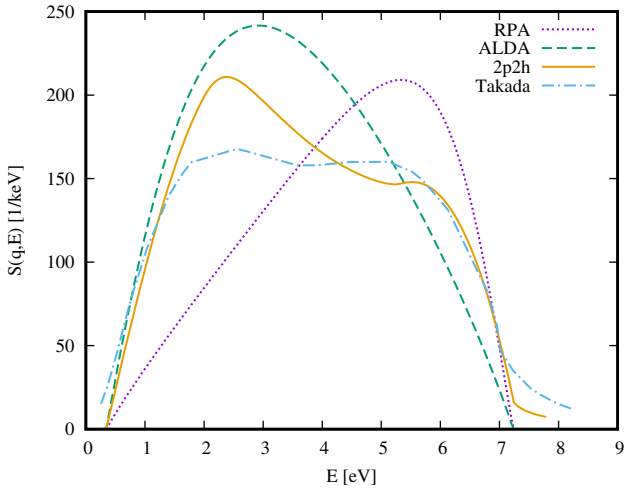

FIG. 2. Dynamic structure factor of the HEG for $r_s = 8$ at $q = 2.2k_F$. $2p2h$ results (yellow continuous curve) are compared with RPA (purple short-dashed curve), ALDA (green long-dashed curve), and with the results of Takada [15] (blue dotted-dashed curve).

different from the RPA: there is a strong shift of spectral weight to lower energies, and a double peak structure appears.

The shift of spectral weight is at the origin of the so-called "ghost plasmon" (called "ghost exciton" in Ref. [15]), which has been introduced by Takayanagi and Lipparini [49] as a pole of the irreducible polarizability on the imaginary axis. It manifests itself through a negative static dielectric function, hence, an attractive screened Coulomb interaction. Such a feature is always absent in the RPA, whereas interestingly, it is present in the ALDA, which, indeed, leads to a strong redshift of spectral weight. Since, for $\omega = 0$ and $q \to 0$, the ALDA approaches the MC result, the onset density for the appearance of the ghost plasmon is the same in both cases. However, the ALDA does not create this effect in the correct way, since there is an overall shift rather than the appearance of an additional low-energy mode. Our $2p2h$ results, instead, yield results that are close to Takada's results in both respects: the shift of oscillator strength, and a (in our result, slightly more intense) distinct low-energy mode, which is to a large extent responsible for the appearance of the ghost plasmon. From an extrapolation of his results up to $r_s = 22$, Takada concludes that it falls always inside the single-pair excitation region. Note that, in 2D ^{3}He, the same low-energy mode has been found below the particle-hole continuum, both theoretically, with the approach used here, and experimentally [50]. Since low-energy modes play an important role in the spectroscopy of correlated systems, the fact that our approach is able to reproduce this phenomenon is an important point.

Another feature of interest is the double plasmon, which can, by definition, only be obtained with a nonadiabatic functional. The result of our HEG $2p2h$ calculations, performed at the density of sodium ($r_s = 4$) and at a wave vector of $q = 0.53/a_0$, is shown in Fig. 1. With respect to the RPA, there is a visible enhancement of oscillator strength in the region of interest with a structure around 12.8 eV, which can be attributed to the double plasmon. This is close to the experimental results of Huotari *et al.* [14] at 12.8 eV, or more recent results [40,41] which suggest 12.5 eV (see inset in Fig. 1). To say more about the significance of this result, in view of the non-negligible differences between sodium and the HEG, we have to move closer to the real system, for which none of the advanced approaches has yet been applied.

Our strategy takes advantage of the Dyson-like linear response equation for χ, which for the HEG can be written in inverse form as

$$f_{\mathrm{xc}}^{\mathrm{hom}}(q,\omega,n) = \frac{1}{\chi_0(q,\omega,n)} - \frac{1}{\chi(q,\omega,n)} - v_c(q). \quad (1)$$

Here, v_c is the Coulomb interaction. The Lindhard function χ_0 contains the information about the noninteracting system, whereas the exchange-correlation kernel $f_{\mathrm{xc}}^{\mathrm{hom}}$ describes interaction effects. Of course, it also depends on the system; i.e., in the case of the HEG $f_{\mathrm{xc}}^{\mathrm{hom}}$ is a function of the density. Still, focusing on f_{xc}, instead of the full χ, allows us to separate materials and interaction effects to a significant extent. Therefore, using the $2p2h$ results for χ, we calculate $f_{\mathrm{xc}}^{\mathrm{hom}}$ for densities ranging from $r_s = 1$ to $r_s = 6$ according to Eq. (1). Only the $q \to 0$ limit is delicate because of lack of precision in the fitting procedure of the MC data. The easiest solution is to correct this limit using the static $f_{\mathrm{xc}}^{\mathrm{CODP}}(q)$ of Corradini *et al.* (COPD) [17], which should be close to exact in the static limit.

The resulting table of $2p2h$ $f_{\mathrm{xc}}^{\mathrm{hom}}$ [31] has now to be used in the real systems: we have to devise the connector. In the case of ground-state calculations, the canonical choice for the exchange-correlation potential $v_{\mathrm{xc}}(\mathbf{r})[n]$ is the LDA, based on the nearsightedness principle [51]. Extensions based on some suitable density average around the local point $\mathbf{r}$ have also been proposed by Gunnarsson *et al.* [52,53]. These authors also provide a length scale for the size of the region over which one should take the average, which is about 2 k_F in reciprocal space. In real space, this corresponds approximately to a radius of 1.6 r_s. The kernel $f_{\mathrm{xc}}(\mathbf{r},\mathbf{r}';\omega)$, however, is nonlocal and at least two regions (around $\mathbf{r}$ and around $\mathbf{r}'$) should give important contributions. Moreover, in the excited states the nearsightedness principle does not apply. This means that the estimate of 1.6 r_s is a lower bound for the region over which one should average, and the pertinent area will, in general, be significantly larger. If it exceeds the scale of the density variation in the system, the canonical approximation should be to take the mean density $\bar{n}$ of the system, rather than a local density. In practice, this means that, in the real system,

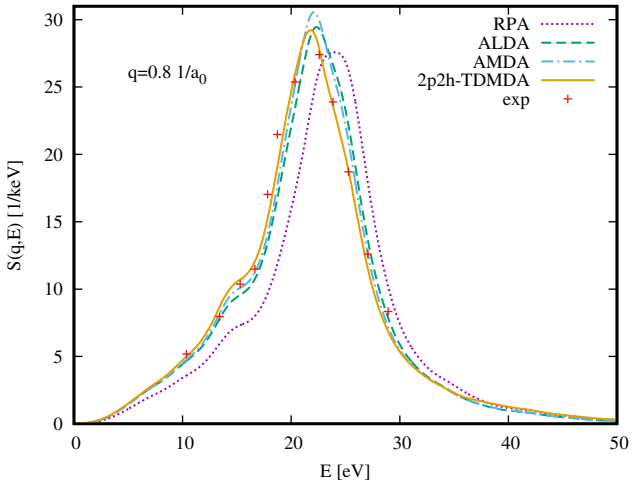

FIG. 3. The dynamic structure factor of silicon at $q = 0.81/a_0$ compared with IXS results of Weissker *et al.* [12]. Curves have the same meaning as in Fig. 4, but additionally, the AMDA result is shown (blue dotted-dashed curve).

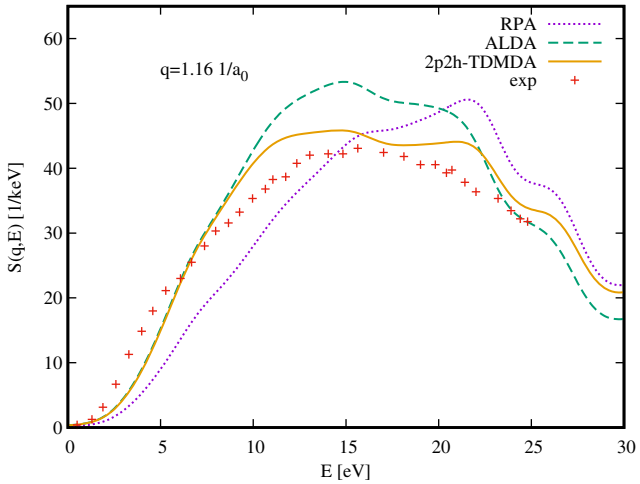

FIG. 4. Similar to Fig. 1, at higher momentum transfer $q = 1.161/a_0$. The homogeneous results are omitted here.

one has to solve the Dyson equation for χ using the inhomogeneous χ_0 and $f_{\mathrm{xc}}^{\mathrm{hom}}$ calculated at the mean density $\bar{n}$ of the real system: this is the time-dependent mean density approximation (TDMDA). Such an approximation is similar in spirit to the $f_{\mathrm{xc}}(\mathbf{q} \to \mathbf{0}; \omega)$ that was derived for the case of small inhomogeneities in [21]. Our arguments point to the fact that it should be valid even when the amplitude of the density variations is large, provided that its real space oscillations are rapid enough. Difficulties should appear whenever off-diagonal elements of f_{xc} become important, e.g., for optical spectra [54]. Considering the interatomic distances in Na with 1.75 r_s and in Si with 2.2 r_s for valence electrons, the TDMDA is well justified for describing the dynamic structure factor in both systems. Therefore, it is applicable in a wider range than previously thought [8,55]. In [32], we illustrate the validity of these arguments by calculations on a 1D model system [56].

In order to get a feeling for whether the choice between the local and the mean density is very delicate, we have calculated spectra for several systems using either the ALDA or the adiabatic mean density approximation (AMDA), which imports from the HEG the same static and local $\delta(\mathbf{r} - \mathbf{r}') f_{\mathrm{xc}}^{\mathrm{hom}}(q \to 0, \omega = 0)$ as does the ALDA, but at the mean, instead of the local, density. In both cases, χ_0 has been calculated using the LDA. For sodium (not shown), the spectra are on top of each other, which is not surprising. More interesting is silicon: it turns out that ALDA and AMDA are still very close, as can be seen in Fig. 3. If there is any difference, the tendency is rather in favor of the AMDA. Although this is merely a snapshot of the local and adiabatic case, it gives evidence that the TDMDA is, at least, a reasonable approximation, and we will adopt it in the following.

With the TDMDA, any sophisticated interpolated or tabulated HEG kernel whatsoever is easy to import and to use in real systems, including nonadiabatic ones. This allows us to calculate sodium again, now using our $2p2h$ kernel. For the ground-state calculation leading to χ_0, we again adopt the LDA. The mean density used in f_{xc} is that of the valence electrons, which are well separated from the core electrons. The result for $q = 0.532 a_0^{-1}$ is given in Fig. 1. The difference with respect to the $2p2h$ homogeneous result is mainly a significant redshift of the main plasmon. Of all the approximations shown, the $2p2h$-TDMDA result has the best agreement with experiment. Since the double plasmon is only accessible by a frequency-dependent kernel, it merits particular attention; therefore, the inset in Fig. 1 shows a zoom. The double plasmon contribution is clearly visible in the experiment and the theory, especially when we remove the Gaussian broadening. The theoretical position is close to the homogeneous result and to experiment, and improves over the pioneering result of Sturm and Gusarov [13] by more than 1 eV.

In order to also probe the impact of the wave vector-dependence of the $2p2h$-TDMDA kernel, Fig. 4 shows results for a larger wave vector, $q = 1.161/a_0$. The $2p2h$-TDMDA result is, again, better than the ALDA. In particular, it includes some lifetime damping. More results and discussions can be found in Ref. [47].

In conclusion, we have built and tabulated an accurate nonlocal and dynamical $2p2h$ exchange-correlation kernel for TDDFT in the HEG, and we have shown that it can be used for the calculation of dynamic structure factors in real solids. The new kernel improves over existing approximations for the HEG, producing, at the same time, double-plasmon and ghost-exciton features that, so far, have been separately obtained through distinct approximations only [15,42]. Moreover, our $2p2h$ kernel can be imported into

real materials through a simple connector that is based on the mean electronic density. This severe approximation precludes its use in the present form in finite systems, and it cannot describe band gaps or bound excitons in insulators. However, it significantly improves the dynamic structure factor of simple metals and semiconductors, including double-plasmon resonances which are completely missed by standard TDDFT approximations. This implies that it could, in principle, also be used to improve many-body perturbation theory based on the screened Coulomb interaction, or total energy calculations using the adiabatic connection [5,6]. Finally, we advocate that the very good quality of these results illustrates a general strategy that is very promising, as it allows one to separate dynamical correlation effects, which can be calculated and tabulated once for all in the HEG [31], from electronic structure features that are material specific but, in principle, easier to deal with.

This research was supported by the European Research Council (ERC Grant Agreement No. 320971), by a Marie Curie FP7 Integration Grant within the 7th European Union Framework Programme and by the Austrian science Fund FWF under Project No. J 3855-N27. Computational time was granted by GENCI (Project No. 544). M. P. wishes to thank M. Vanzini and J. Sky for providing input files and H. Böhm for fruitful discussions.

*martin.panholzer@jku.at

[1] W. Schülke, *Electron Dynamics by Inelastic X-Ray Scattering*, Oxford Series on Synchrotron Radiation (Oxford University Press, New York, 2007).
[2] G. Was, *Fundamentals of Radiation Materials Science: Metals and Alloys* (Springer, Berlin, 2007).
[3] G. Onida, L. Reining, and A. Rubio, Rev. Mod. Phys. **74**, 601 (2002).
[4] S. Maier, *Plasmonics: Fundamentals and Applications* (Springer, New York, 2007).
[5] O. Gunnarsson and B. I. Lundqvist, Phys. Rev. B **13**, 4274 (1976).
[6] D. C. Langreth and J. P. Perdew, Phys. Rev. B **15**, 2884 (1977).
[7] R. Martin, L. Reining, and D. Ceperley, *Interacting Electrons: Theory and Computational Approaches* (Cambridge University Press, Cambridge, England, 2016).
[8] S. Botti, A. Schindlmayr, R. D. Sole, and L. Reining, Rep. Prog. Phys. **70**, 357 (2007).
[9] C. Verdi, F. Caruso, and F. Giustino, Nat. Commun. **8**, 15769 (2017).
[10] C. Rödl, K. O. Ruotsalainen, F. Sottile, A.-P. Honkanen, J. M. Ablett, J.-P. Rueff, F. Sirotti, R. Verbeni, A. Al-Zein, L. Reining, and S. Huotari, Phys. Rev. B **95**, 195142 (2017).
[11] S. Rahman and G. Vignale, Phys. Rev. B **30**, 6951 (1984).
[12] H.-C. Weissker, J. Serrano, S. Huotari, E. Luppi, M. Cazzaniga, F. Bruneval, F. Sottile, G. Monaco, V. Olevano, and L. Reining, Phys. Rev. B **81**, 085104 (2010).
[13] C. Sternemann, S. Huotari, G. Vankó, M. Volmer, G. Monaco, A. Gusarov, H. Lustfeld, K. Sturm, and W. Schülke, Phys. Rev. Lett. **95**, 157401 (2005).
[14] S. Huotari, C. Sternemann, W. Schülke, K. Sturm, H. Lustfeld, H. Sternemann, M. Volmer, A. Gusarov, H. Müller, and G. Monaco, Phys. Rev. B **77**, 195125 (2008).
[15] Y. Takada, Phys. Rev. B **94**, 245106 1 (2016).
[16] M. Petersilka, U. J. Gossmann, and E. K. U. Gross, Phys. Rev. Lett. **76**, 1212 (1996).
[17] M. Corradini, R. Del Sole, G. Onida, and M. Palummo, Phys. Rev. B **57**, 14569 (1998).
[18] P. E. Trevisanutto, A. Terentjevs, L. A. Constantin, V. Olevano, and F. D. Sala, Phys. Rev. B **87**, 205143 (2013).
[19] E. K. U. Gross and W. Kohn, Phys. Rev. Lett. **55**, 2850 (1985).
[20] L. A. Constantin and J. M. Pitarke, Phys. Rev. B **75**, 245127 (2007).
[21] V. U. Nazarov, G. Vignale, and Y.-C. Chang, Phys. Rev. Lett. **102**, 113001 (2009).
[22] L. Reining, V. Olevano, A. Rubio, and G. Onida, Phys. Rev. Lett. **88**, 066404 (2002).
[23] S. Botti, F. Sottile, N. Vast, V. Olevano, L. Reining, H.-C. C. Weissker, A. Rubio, G. Onida, R. Del Sole, and R. W. Godby, Phys. Rev. B **69**, 155112 (2004).
[24] S. Sharma, J. K. Dewhurst, A. Sanna, and E. K. U. Gross, Phys. Rev. Lett. **107**, 186401 (2011).
[25] S. Rigamonti, S. Botti, V. Veniard, C. Draxl, L. Reining, and F. Sottile, Phys. Rev. Lett. **114**, 146402 (2015).
[26] V. U. Nazarov, I. V. Tokatly, S. Pittalis, and G. Vignale, Phys. Rev. B **81**, 245101 (2010).
[27] Z. Qian and G. Vignale, Phys. Rev. B **65**, 235121 (2002).
[28] S. Conti, R. Nifosì, and M. P. Tosi, J. Phys. Condens. Matter **9**, L475 (1997).
[29] C. F. Richardson and N. W. Ashcroft, Phys. Rev. B **50**, 8170 (1994).
[30] W. Kohn and L. J. Sham, Phys. Rev. **140**, A1133 (1965).
[31] The tabulated $2p2h$ kernel is available at: https://etsf.polytechnique.fr/research/connector/2p2h-kernel. Some results are shown in the Supplemental Material for illustration [32].
[32] See Supplemental Material at http://link.aps.org/supplemental/10.1103/PhysRevLett.120.166402 for theoretical and computational details and for additional results, which includes Refs. [33–39].
[33] M. Casula, S. Sorella, and G. Senatore, Phys. Rev. B **74**, 245427 (2006).
[34] X. Gonze, G.-M. Rignanese, M. Verstraete, J.-M. Beuken, Y. Pouillon, R. Caracas, F. Jollet, M. Torrent, G. Zerah, M. Mikami *et al.*, Z. Kristallogr. **220**, 558 (2005).
[35] See www.dp-code.org.
[36] N. Troullier and J. L. Martins, Phys. Rev. B **43**, 1993 (1991).
[37] H. J. Monkhorst and J. D. Pack, Phys. Rev. B **13**, 5188 (1976).
[38] D. R. Hamann, Phys. Rev. B **40**, 2980 (1989).
[39] Y. Okada and Y. Tokumaru, J. Appl. Phys. **56**, 314 (1984).
[40] M. Cazzaniga, H.-C. Weissker, S. Huotari, T. Pylkkänen, P. Salvestrini, G. Monaco, G. Onida, and L. Reining, Phys. Rev. B **84**, 075109 (2011).

[41] S. Huotari, M. Cazzaniga, H. C. Weissker, T. Pylkkanen, H. Muller, L. Reining, G. Onida, and G. Monaco, Phys. Rev. B **84**, 075108 (2011).
[42] K. Sturm and A. Gusarov, Phys. Rev. B **62**, 16474 (2000).
[43] H. M. Böhm, R. Holler, E. Krotscheck, and M. Panholzer, Phys. Rev. B **82**, 224505 (2010).
[44] J. W. Clark, L. R. Mead, E. Krotscheck, K. E. Kürten, and M. L. Ristig, Nucl. Phys. **A328**, 45 (1979).
[45] E. Krotscheck and J. W. Clark, Nucl. Phys. **A328**, 73 (1979).
[46] P. Gori-Giorgi, F. Sacchetti, and G. B. Bachelet, Phys. Rev. B **61**, 7353 (2000).
[47] M. Panholzer, M. Gatti, and L. Reining (to be published).
[48] M. Lein, E. K. U. Gross, and J. P. Perdew, Phys. Rev. B **61**, 13431 (2000).
[49] K. Takayanagi and E. Lipparini, Phys. Rev. B **56**, 4872 (1997).
[50] H. Godfrin, M. Meschke, H.-J. Lauter, A. Sultan, H. M. Böhm, E. Krotscheck, and M. Panholzer, Nature (London) **483**, 576 (2012).
[51] W. Kohn, Phys. Rev. Lett. **76**, 3168 (1996).
[52] O. Gunnarsson, M. Jonson, and B. Lundqvist, Solid State Commun. **24**, 765 (1977).
[53] O. Gunnarsson, M. Jonson, and B. I. Lundqvist, Phys. Rev. B **20**, 3136 (1979).
[54] F. Sottile, M. Marsili, V. Olevano, and L. Reining, Phys. Rev. B **76**, 161103 (2007).
[55] In the case of finite systems, this idea has, obviously, to be adapted, for example, by using a jellium sphere as reference for a cluster.
[56] M. Panholzer, J. Low Temp. Phys. **187**, 639 (2017).